Simultaneous compensation for aberration and axial elongation in three-dimensional laser nanofabrication by a high numerical-aperture objective

Benjamin. P. Cumming,[1] **Sukanta Debbarma,**[2] **Barry Luther-Davis,**[2] **and Min Gu**[1,*]

[1]*Centre for Micro-Photonics and CUDOS, Faculty of Engineering and Industrial Sciences, Swinburne University of Technology, Hawthorn, Australia*
[2]*Laser Physics Centre and CUDOS, Research School of Physical Sciences and Engineering, Australian National University, Canberra, Australia*

[*] *mgu@swin.edu.au*

Abstract: One of the challenges in laser direct writing with a high numerical-aperture objective is the severe axial focal elongation and the pronounced effect of the refractive-index mismatch aberration. We present the simultaneous compensation for the refractive-index mismatch aberration and the focal elongation in three-dimensional laser nanofabrication by a high numerical-aperture objective. By the use of circularly polarized beam illumination and a spatial light modulator, a complex and dynamic slit pupil aperture can be produced to engineer the focal spot. Such a beam shaping method can result in circularly symmetric fabrication along the lateral directions as well as the dynamic compensation for the refractive-index mismatch aberration even when the laser beam is focused into the material of a refractive index up to 2.35.

OCIS codes: (220.1080) Active or adaptive optics; (220.1000) Aberration compensation; (220.4241) Nanostructure fabrication.

References and links

1. P. Török, P. Varga, Z. Laczik, and G. R. Booker, "Electromagnetic diffraction of light focused through a planar interface between materials of mismatched refractive indexes–an integral-representation," J. Opt. Soc. Am. A **12,** 325–332 (1995).
2. M. Gu, *Advanced Optical Imaging Theory* (Springer, Heidelberg, 2000).
3. I. Staude, G. von Freymann, S. Essig, K. Busch, and M. Wegener, "Waveguides in three-dimensional photonic-bandgap materials by direct laser writing and silicon double inversion," Opt. Lett. **36,** 67–69 (2011).
4. E. Nicoletti, D. Bulla, B. Luther-Davies, and M. Gu, "Wide-angle stop-gap chalcogenide photonic crystals generated by direct multiple-line laser writing," Appl. Phys. B **105,** 847–850 (2011).
5. S. Wong, M. Deubel, F. Pérez-Willard, S. John, G.A. Ozin, M. Wegener, and G. von Freymann, "Direct laser writing of three-dimensional photonic crystals with a complete photonic bandgap in chalcogenide glasses," Adv. Mat. **18,** 265–269 (2006).
6. K.C. Vishnubhatla, N. Bellini, R. Ramponi, G. Cerullo, and R. Osellame, "Shape control of microchannels fabricated in fused silica by femtosecond laser irradiation and chemical etching," Opt. Express **17,** 8685–8695 (2009).
7. F. He, Y. Cheng, J. Lin, J. Ni, Z. Xu, K. Sugioka, and K. Midorikawa, "Independent control of aspect ratios in the axial and lateral cross sections of a focal spot for three-dimensional femtosecond laser micromachining," New J. Phys. **13,** 083014 (2011).

#190384 - $15.00 USD Received 10 May 2013; revised 20 Jul 2013; accepted 22 Jul 2013; published 5 Aug 2013

8. M. Martinez–Corral, C. Ibáñez-López, G. Saavedra, and M. Caballero, "Axial gain resolution in optical sectioning fluorescence microscopy by shaded-ring filters," Opt. Express **11,** 1740–1745 (2003).
9. H. Lin, B. Jia, and M. Gu, "Generation of an axially super-resolved quasi-spherical focal spot using an amplitude-modulated radially polarized beam," Opt. Lett. **36,** 2471–2473 (2011).
10. R. Osellame, S. Taccheo, M. Marangoni, R. Ramponi, P. Laporta, D. Polli, S. De Silvestri, and G. Cerullo, "Femtosecond writing of active optical waveguides with astigmatically shaped beams," J. Opt. Soc. Am. B **20,** 1559–1567 (2003).
11. Y. Cheng, K. Sugioka, K. Midorikawa, M. Masuda, K. Toyoda, M. Kawachi, and K. Shihoyama, "Control of the cross-sectional shape of a hollow microchannel embedded in photostructurable glass by use of a femtosecond laser," Opt. Lett. **28,** 55–57 (2003).
12. M. Ams, G. Marshall, D. Spence, and M. Withford, "Slit beam shaping method for femtosecond laser direct-write fabrication of symmetric waveguides in bulk glasses," Opt. Express **13,** 5676–5681 (2005).
13. P. S. Salter, A. Jesacher, J. B. Spring, B. J. Metcalf, N. Thomas-Peter, R. D. Simmonds, N. K. Langford, I. A. Walmsley, and M. J. Booth, "Adaptive slit beam shaping for direct laser written waveguides," Opt. Lett. **37,** 470–472 (2012).
14. C. Mauclair, A. Mermillod-Blondin, N. Huot, E. Audouard, and R. Stoian, "Ultrafast laser writing of homogeneous longitudinal waveguides in glasses using dynamic wavefront correction," Opt. Express **16,** 5481–5492 (2008).
15. A. Jesacher, G. D. Marshall, T. Wilson, and M. J. Booth, "Adaptive optics for direct laser writing with plasma emission aberration sensing," Opt. Express **18,** 656–661 (2010).
16. R. D. Simmonds, P. S. Salter, A. Jesacher, and M. J. Booth, "Three dimensional laser microfabrication in diamond using a dual adaptive optics system," Opt. Express **19,** 24122–24128 (2011).
17. B. P. Cumming, A. Jesacher, M. J. Booth, T. Wilson, and M. Gu, "Adaptive aberration compensation for three-dimensional micro-fabrication of photonic crystals in lithium niobate," Opt. Express **19,** 9419–9425 (2011).
18. B. P. Cumming, S. Debbarma, B. Luther-Davies, and M. Gu, "Effect of refractive index mismatch aberration in arsenic trisulfide," Appl. Phys. B **109,** 227–232 (2012).
19. E. H. Waller, M. Renner, and G. von Freymann, "Active aberration- and point-spread-function control in direct laser writing," Opt. Express **20,** 24949–24956 (2012).

1. Introduction

The fabrication of three-dimensional (3D) photonic nanostructures by use of a femtosecond laser beam focused by a high numerical-aperture (NA) objective is often hindered by the complicated focal asymmetry [1, 2]. First, an axial focal elongation induced by the limited NA of the focusing objective can lead to a focal asymmetry with respect to the transverse direction. Second, in the presence of the mismatch of the refractive-indices between the immersion medium of a high NA objective and the material where nanophotonic structures are fabricated, the axial elongation is accompanied by an axial asymmetry with strong side lobes along one axial direction. Third, the depolarization effect of a high NA objective can cause an in-plane focal asymmetry with respect to the orientation of the incident beam polarization. Both the refractive-index mismatch spherical aberration and the depolarization become stronger when the NA approaches 1.4 which is necessary for the nanofabrication. Accordingly, such a strongly asymmetric focal spot often results in an axial resolution that is significantly poorer than the lateral resolution in direct laser writing (DLW) and can lead to unwanted optical effects such as linear birefringence in DLW-generated photonic crystal waveguides [3] and a lack of a complete photonic band-gap [4, 5].

To compensate for the axial focal elongation, one has developed multi-line DLW [5, 6], complex spatial filtering [7–9], and astigmatic [10] and slit-beam shaping [11–13] methods. While these methods can improve the aspect ratio of the focal spot in the transverse and axial directions, their effect on compensating for the refractive-index mismatching have not been explored. Although a spatial light modulator (SLM) slit-beam method was employed for the compensation for the axial focal elongation in DLW of NA 0.5 [13], no compensation for the refractive-index mismatch aberration and depolarization has been studied. On the other hand, adaptive optics based on an SLM, in which case aberrated wavefronts can be compensated by the SLM-generated conjugated phase, has been developed without taking the axial focal elongation into

#190384 - $15.00 USD Received 10 May 2013; revised 20 Jul 2013; accepted 22 Jul 2013; published 5 Aug 2013

consideration [14–19].

In this work we show a complex and dynamic slit beam shaping method using an SLM to simultaneously compensate for the axial focal elongation and the refractive-index mismatch aberration. The difference of our method from the SLM slit beam shaping method reported recently [13] is that our adjustible slit has a complex phase function to compensate for the refractive-index mismatch aberration that is dependent on the depth of the focal position in the medium where DLW is performed with a high NA objective. In addition, instead of using a linearly polarized beam, which can cause an in-plane polarization-dependent focal asymmetry when a slit rotates for the fabrication of a curved or bent structure, we use a circularly polarized beam. As such, we demonstrate that sub-micrometer nanowires can be generated with a highly circularly symmetric focal spot when the elongation and aberration are compensated simultaneously even in the fabrication material that have a refractive index of up to 2.35.

2. High numerical aperture slit beam-shaping

Let us consider a slit-shaped aperture with an orientation angle of θ placed at the back focal plane of an objective, as depicted in Figs. 1(a) and 1(b). At the focus, the size of the focal spot in the constricted direction is increased due to the reduced aperture size of the slit. By an appropriate choice of the slit width W, the transverse focal spot size can be enlarged by the restriction of the slit width to an extent that it matches the axially elongated focal spot size. Consequently, the focusing of a slit shaped beam can produce a vertical disk shaped intensity point spread function (IPSF) oriented perpendicular to the slit as shown in Fig. 1(b).

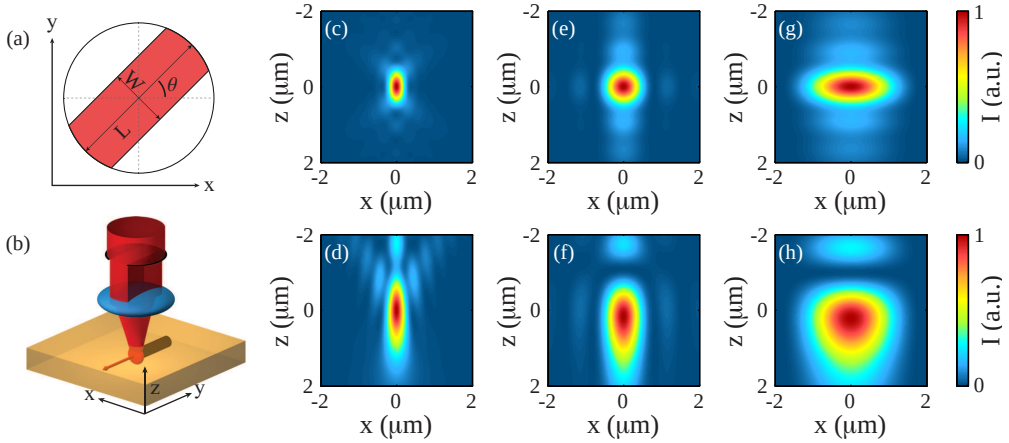

Fig. 1. (a) Definition of a slit shaped beam. (b) Focusing of a slit-shaped beam by an objective lens. The images in (c-h) are normalized calculated IPSFs in the ZX plane under various conditions. (c-d) are calculated with the full objective aperture (W = 1) whilst (e-f) and (g-h) are calculated with slit widths of W = 1.76 mm and 0.76 mm, respectively. (c), (e) and (g) assume the aberration-free condition, whilst (d), (f) and (g) are calculated in the presence of the refractive-index mismatch aberration when a laser beam is focused to a depth of 60 μm.

Although the slit beam shaping method has been applied to the case of low NA DLW [11–13] at a micrometer scale, it is necessary to adopt a high NA objective for nanofabrication, in which case a phase-modulated slit aperture whose transmittance is a complex function is needed. To keep the rotatory symmetry of the disk-like focal spot produced by a high NA objective, we use circularly polarization illumination instead of a linearly polarized beam.

#190384 - $15.00 USD Received 10 May 2013; revised 20 Jul 2013; accepted 22 Jul 2013; published 5 Aug 2013

Figures 1(c)-1(h) show the normalized XZ cross sections of the calculated IPSF when a circularly polarized beam is focused under various conditions. The calculations were performed with a vectorial Debye integral [1, 2, 17, 18] for a slit like beam defined by Fig. 1(a). The NA of the objective in the calculation was 1.4, and its immersion medium of refractive index 1.52 was used. The incident wave was right circularly polarized with a wavelength of 800 nm. The slit length L was set to 5.04 mm to match the diameter of the objectives back aperture.

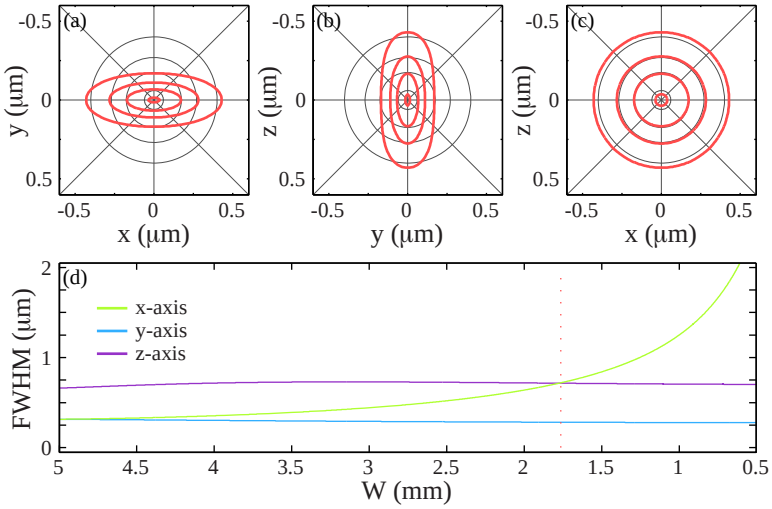

Fig. 2. Contour plots of the IPSF in the (a) XY, (b) ZY and (c) ZX planes at normalized intensity levels of 0.5, 0.75, 0.9 and 0.995. (d) Evolution of the FWHM on the x-, y- and z-axes as a function of W when the slit is parallel to the y-axis. The red dotted line corresponds to the location of circular symmetry.

Figure 1(c) shows the IPSF when focusing to a depth of 60 μm in an isotropic polymer (IP-L - Nanoscribe GmbH) and when utilizing the full objective aperture ($W = 1$). The polymer has a refractive index of 1.48 and the spherical aberration was assumed to be compensated when the phase of the slit transmittance is conjugated according to the refractive-index mismatch aberration [1, 2]. Figure 1(e) shows the IPSF when the slit width is limited to an optimal width of $W = 1.76$ mm, aligned parallel to the y-axis. The IPSF broadens along the x-axis to form a circularly symmetric focal distribution in the ZX plane. The peak intensity of the focus is lower than the full aperture case by a factor of 5.4 due to both the reduced transmission of the slit and the larger volume of the focus. The further reduction of the slit width can lead to the destruction of circular symmetry in the XZ plane as shown in Fig. 1(g) where a slit width of $W = 0.76$ mm is applied.

Figures 1(d), 1(f) and 1(h) show the cases when no aberration compensation is applied. For a focal depth of 60 μm the additional aberration induced focal elongation necessitates a smaller slit width of $W = 0.76$ mm to achieve an aspect ratio of 1 in the ZX plane. However, note that the presence of the aberration destroys the circular symmetry of the focus and that the resolution of the focus is significantly poorer than when the slit transmittance is conjugated according to the refractive-index mismatch aberration (Fig. 1(e)). It is therefore vital for aberration compensation to be employed simultaneously with the slit beam shaping if circular symmetry is to be achieved.

The high degree of the circular symmetry of the aberration compensated dynamic slit method and the disk like shape of the focus are illustrated in the calculated contour plots shown in Figs.

#190384 - $15.00 USD Received 10 May 2013; revised 20 Jul 2013; accepted 22 Jul 2013; published 5 Aug 2013

2(a)-2(c). Figure 2(d) also shows the evolution of the full width at half maximum (FWHM) of the IPSF as a function of W under the aberration free condition. The FWHM in the x-axis increases dramatically as the slit width is lowered whilst the FWHMs of the y- and z-axis remain mostly constant. At W = 1.76 mm the x-axis and z-axis FWHMs cross and a circularly symmetric aspect ratio of 1 is achieved. The consistency of the axial FWHM shows that the 3D resolution is uncompromised by this method whilst the independence of the FWHMs on the focal depth permit the 1.76 mm optimal slit to achieve a circularly symmetric focus at any focal depth.

3. Dynamic SLM based slit beam shaping

The principle of generating a phase modulated adaptive slit shaped beam by a phase only SLM is shown in Fig. 3(a). A phase grating is utilized to separate the first order diffraction term from the remainder of the wavefront whilst the conjugated function related to the refractive-index mismatch is added for aberration compensation. An adjustable slit shape is then superposed onto the phase pattern such that the total phase modulation is limited to a slit shape [13]. By imaging the surface of the SLM to the back aperture of the objective lens with a 4f imaging system as shown in Fig. 3(b), the portions of the wavefront without the phase grating can be filtered with a simple pinhole such that only the slit shaped first order diffraction is permitted to transmit to the objective lens [13].

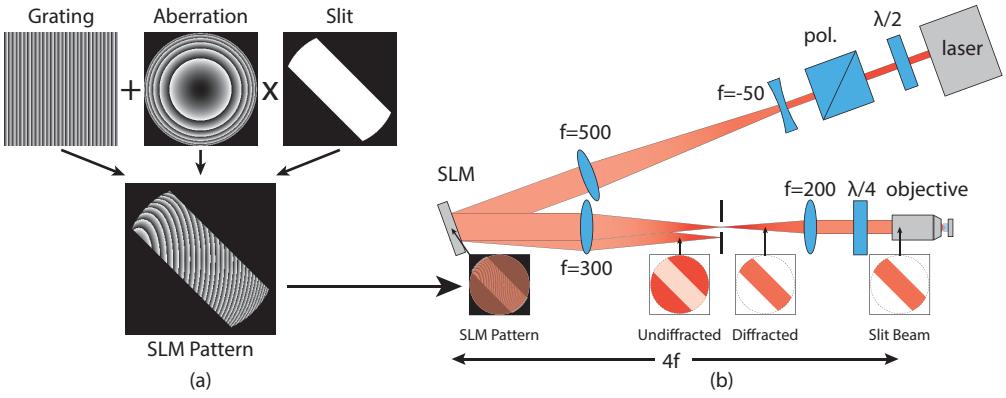

Fig. 3. (a) Phase pattern generation (b) Experimental setup for simultaneous compensation of aberration and axial elongation with a phase only SLM.

The size, shape and angle of the slit shaped beam at the back aperture of the objective can then be dynamically changed during fabrication by simply altering the region of the SLM that displays the phase ramp. In addition, the refractive-index mismatch aberration can by dynamically updated simultaneously by adjusting the compensation pattern to the conjugate of the phase at any given fabrication depth. This work utilized a Boulder Nonlinear Systems SLM (HSPDM5120785-PCIe) for phase modulation illuminated with an ultrafast laser amplifier (Libra HE, Coherent Scientific) with an operating wavelength of 800 nm, a pulse width of 100 fs and a repetition rate of 10 kHz. A 1.4 NA objective lens (Olympus UPLANSAPO 100 XO) is utilized to focus the laser beam.

4. Symmetric nanofabrication

Experimental verification of circularly symmetric nanofabrication can be seen in the scanning electron microscope (SEM) images of fabricated IP-L polymer nanowires in Fig. 4(b) and 4(c),

#190384 - $15.00 USD Received 10 May 2013; revised 20 Jul 2013; accepted 22 Jul 2013; published 5 Aug 2013

where the full objective aperture and optimized slit width cases are shown, respectively. The length of the nanowires runs into the page and the laser propagated from the top of the images as shown by the diagram in Fig 4(a).

The nanowires were fabricated by creating a 60 μm thick film of the IP-L polymer between two glass coverslips. As the refractive index of the polymer (n_2= 1.48) is lower than the refractive index of the immersion medium (n_1= 1.52), spherical aberration caused by the refractive-index mismatch is imparted onto the laser wavefront [1, 2] and hence simultaneous compensation via the phase only SLM is required. The precise level of aberration compensation that was required was found via an adaptive axial response method reported elsewhere [18]. The nanowires were fabricated in the power range between 15 and 25 μW and the power was scaled each time so that approximately equal peak intensity was maintained for each slit width. The fabrication speed was 5 μm/s and the rods protruded 1 μm out from the polymer supporting structure. In experiment, the optimal slit width for an aspect ratio of 1 was found to be W = 1.16 mm (Fig. 4(c)), which is between 1.76 mm and 0.76 mm as predicted by the theoretical calculations. The reason for the narrower slit width is the presence of system aberration which distorts the focus in addition to the spherical aberration produced by the refractive-index mismatch.

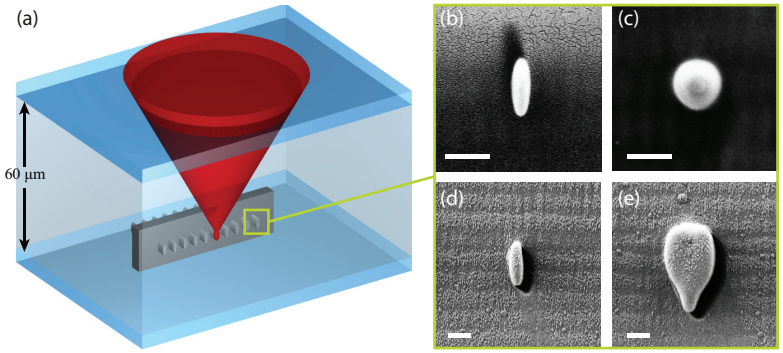

Fig. 4. (a) Diagram of nanowire fabrication. (b-e) End view of polymer nanowires fabricated with (a) full objective aperture and (b) slit beam shape for the case of an aberration compensated beam. (c) and (d) show the full aperture and slit beam cases, respectively, for the case of an aberrated beam. The length of the rods runs into the page and the scale bars are 1 μm.

The effect of the spherical aberration on the nanowire symmetry was also observed when fabricating nanowires without the simultaneous compensation for the refractive-index mismatch aberration. Figures 4(d) and 4(e) show the cases of the full objective aperture and slit width of W = 0.23, respectively, for an uncompensated beam. The additional elongation from the aberration prohibits a unit aspect ratio from being achieved, and the circular symmetry is also destroyed in agreement with the numerical calculations.

Finally, we apply our method into the chalcogenide glass arsenic trisulfide (As_2S_3) [4, 5, 18] which has a refractive index of 2.35. The elongation of the focus when focusing within As_2S_3 is a factor of 2.2 times larger at the diffraction limit in comparison to the IP-L polymer, and the magnitude of the refractive-index mismatch aberration is over an order of magnitude higher. Whilst As_2S_3 is a highly photosensitive and nonlinear material, these properties were not observed to influence the dynamics of the slit method and so no additional control of the fabrication power or phase compensation was required.

Simple curved structures were fabricated at different depths as shown in Fig. 5(a). Figure 5(b)

#190384 - $15.00 USD Received 10 May 2013; revised 20 Jul 2013; accepted 22 Jul 2013; published 5 Aug 2013

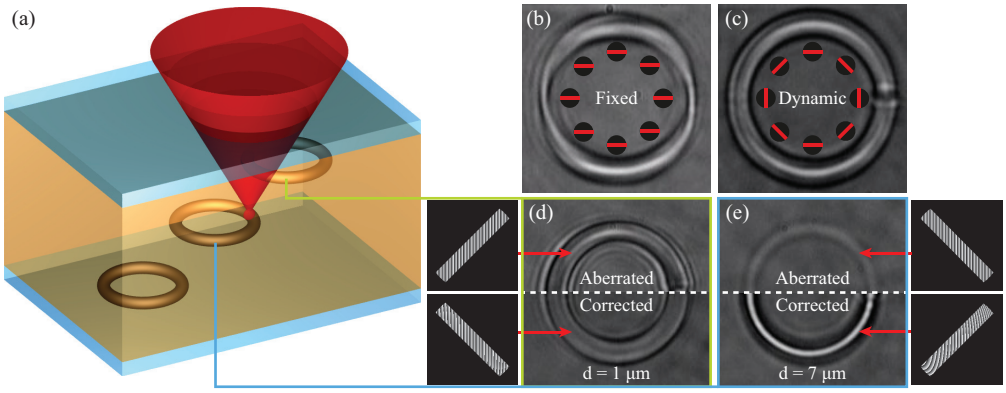

Fig. 5. (a) Diagram of dynamic ring fabrication. (b) and (c) show top view optical images of circular trajectories fabricated in As_2S_3 with fixed and dynamic slit angles, respectively. The inset images show the slit angle at each point of the trajectory. (d) and (e) show the same circular trajectories fabricated at depths of 1 μm and 7 μm, respectively, both with and without simultaneous compensation of aberration. The diameter of the circles is 10 μm and example phase patterns are shown for each case. Images of the corresponding compensation patterns are also shown.

shows wide field optical images of the curved structures fabricated with a fixed slit whilst Fig. 5(c) shows the improvement when a dynamic slit angle is applied. The effect of the refractive-index mismatch aberration and its simultaneous compensation via the SLM can be seen in Figs. 5(d) and 5(e) where structures are fabricated at depths of 1 μm and 7 μm , respectively. The aberrated structures deviate significantly from the corrected structures as the depth is increased. It should be noted that the apparent deterioration of the corrected case is due to the lack of aberration compensation in the wide field imaging system and hence the image quality deteriorates when imaging all structures. Nonetheless, a clear improvement is observed when both the axial elongation and refractive-index mismatch aberration are simultaneously compensated.

5. Conclusion

We have demonstrated the simultaneous compensation for the spherical aberration caused by the refractive-index mismatch and the elongation in DLW with a high NA objective. As a result, symmetric nanostructures with a unit aspect ratio can be fabricated into a material with refractive index up to 2.35 by the use of a complex and dynamic slit generated by the SLM. We have shown that the slit can be dynamically updated at high speed for application that requires symmetric nanofabrication across a range of fabrication directions.

Acknowledgments

This research was supported by the Australian Research Council Centre of Excellence for Ultrahigh bandwidth Devices for Optical Systems (project number CE110001018).

#190384 - $15.00 USD Received 10 May 2013; revised 20 Jul 2013; accepted 22 Jul 2013; published 5 Aug 2013